Invited Paper

Sensitive far-IR survey spectroscopy: BLISS for SPICA

C.M. Bradford[a], Matt Kenyon[a], Warren Holmes[a], James Bock[a], Timothy Koch,[a] and the BLISS study team[b]

[a]Jet Propulsion Laboratory, Caltech, Pasadena, CA;

ABSTRACT

We present a concept for BLISS, a sensitive far-IR-submillimeter spectrograph for SPICA. SPICA is a JAXA-led mission featuring a 3.5-meter telescope actively cooled to below 5K, envisioned for launch in 2017. The low-background platform is especially compelling for moderate-resolution survey spectroscopy, for which BLISS is designed. The BLISS / SPICA combination will offer line sensitivities below $10^{-20}\,\mathrm{W\,m^{-2}}$ in modest integrations, enabling rapid survey spectroscopy of galaxies out to redshift 5. The far-IR fine-structure and molecular transitions which BLISS / SPICA will measure are immune to dust extinction, and will unambiguously reveal these galaxies' redshifts, stellar and AGN contents, gas properties, and heavy-element abundances. Taken together, such spectra will reveal the history of galaxies from 1 GY after the Big Bang to the present day. BLISS is comprised of five sub-bands, each with two $R \sim 700$ grating spectrometer modules. The modules are configured with polarizing and dichroic splitters to provide complete instantaneous spectral coverage in two sky positions. To approach background-limited performance, BLISS detectors must have sensitivities at or below $5 \times 10^{-20}\,\mathrm{W\,Hz^{-1/2}}$, and the format is 10 arrays of several hundred pixels each. It is anticipated that these requirements can be met on SPICA's timescale with leg-isolated superconducting (TES) bolometers cooled with a 50 mK magnetic refrigerator.

Keywords: SPICA, spectroscopy, far-IR, BLISS, bolometers

1. INTRODUCTION

We are developing concepts for a sensitive far-IR spectrograph called BLISS which could be contributed by the US to the SPICA. The SPICA (Space Infrared Telescope for Cosmology and Astrophysics) mission is a 3.5-meter telescope actively cooled to below 5 K, and is planned for launch to an Earth-Sun L2-point orbit in 2017. SPICA is led by JAXA, but a substantial contribution from ESA is under study. SPICA and its instruments are described in SPIE conference 7010, co-extant with this conference.[1–3] The BLISS (Background-Limited Infrared-Submillimeter Spectrometer) instrument is a broadband grating spectrometer coupled to sensitive bolometers. The wavelength range of BLISS is under study but currently baselined as 38 to 430 μm, the range for which SPICA can be a powerful complement to the other facilities, particularly JWST & ALMA. Sensitive far-IR spectroscopy from space remains a true frontier in astrophysics. The combination of BLISS with the cold SPICA telescope can offer 4–5 orders of magnitude sensitivity improvement in over the currently-planned facilities in this wavelength range, bringing it on par with the optical/near-IR and radio spectral ranges. We provide here an update on the previous SPIE proceeding on BLISS.[4] In the last two years, the science case has sharpened, the technology has matured, and the BLISS instrument concept has been refined in light of the resources available on SPICA. We revisit the scientific case, outline the BLISS instrument and system considerations, and present progress on the key technology: the ultrasensitive TES bolometers.

2. SCIENTIFIC MOTIVATION

After the Cosmic Microwave Background (CMB) is accounted for, the remaining cosmic background light is the integrated emission from all stars and galaxies since they began forming. The spectrum of this cosmic background

Send correspondence to CMB: e-mail: matt.bradford@jpl.nasa.gov, phone: 818 393 7499
BLISS Study Team: authors above plus P. Day, H. Nguyen, M. Werner, R. Cofield, C. Paine, JPL; K. Irwin, NIST; M. Harwit, G. Stacey, Cornell U.; G. Helou, L. Armus, Caltech; J.D. Smith, U. Toledo; S. Chapman, Cambridge; G. Rieke U. Arizona; D. Lester, U. Texas; ; T. Nakagawa, H. Matsuhara, ISAS / JAXA; T. Onaka, U. Tokyo; H. Shibai, Nagoya U.; M. Tamura, NAOJ

Millimeter and Submillimeter Detectors and Instrumentation for Astronomy IV
edited by William D. Duncan, Wayne S. Holland, Stafford Withington, Jonas Zmuidzinas
Proc. of SPIE Vol. 7020, 70201O, (2008) · 0277-786X/08/$18 · doi: 10.1117/12.790156

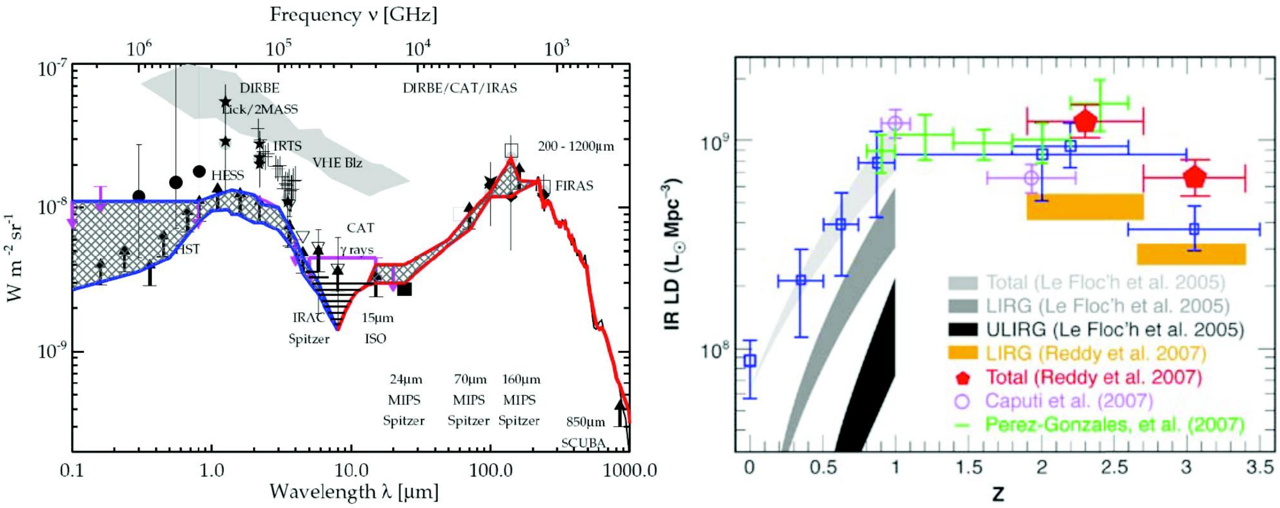

Figure 1. LEFT: Observational constraints on the intensity of the cosmic background radiation from radio to ultraviolet wavelengths, reprinted from Dole et al. (2006). The two peaks, one in the optical/near-IR and one in the far-IR, have comparable energy density. This implies that half of the energy released throughout the history of stars and galaxies is absorbed by dust. RIGHT: The infrared luminosity density as a function of redshift to z = 3.5 (taken from Reddy et al. 2007). The blue points represent pre-/non-Spitzer data. The Spitzer-based data include results from Reddy et al. (2007), Caputi et al. (2007), Prez-Gonzlez et al. (2005), Le Floch et al. (2005). The bands indicate the total, LIRG, and ULIRG contribution to the total infrared luminosity density at z ¡ 1, as determined by Le Floch et al.

shows two broad peaks, one at $\sim$1 μm, and one at $\sim$150 μm. The long-wavelength component, called the Cosmic Infrared Background (CIB), is produced by dust heated by nearby stars or accretion phenomena. The fact that the energy in this dust component is comparable to that in the optical / near-IR component means that on average in the universe, interstellar dust has absorbed and reradiated half of the total energy ever generated by stars and black-hole accretion. This dust-enshrouded component must be included for a complete history of stellar nucleosynthesis and galaxy evolution and there is evidence that the galaxies which produce the CIB may be different from those that produce the optical / near-IR background. The first high-redshift dusty sources discovered appear to have properties similar to those of the local luminous and ultraluminous IR galaxies (LIRGs and ULIRGs): very powerful galaxies so highly obscured that they emit more than 90% of their luminosity in the far-IR. The next generation of continuum surveys will discover tens of thousands of similar galaxies at redshifts of 1–5 as the bulk of the CIB is resolved into its constituent sources.

The key to studying these galaxies will be spectroscopy at long-wavelengths. The rest frame mid-to-far-IR offers a rich suite of tools immune to dust extinction that probe all phases of the interstellar medium: ionized, neutral atomic, and molecular. Measurement of these gas-phase and solid-state features provides redshifts, gas masses, and physical conditions from which luminosities, stellar populations, and star formation histories are derived. With the spectrometers on the airborne observatories and the Infrared Space Observatory (ISO), astronomers have developed far-IR tools and used them to reveal the processes inside a small handful of nearby galaxies. Now Spitzer and soon Herschel will enable mid- to far-IR spectroscopy of bright galaxies to $z \sim 0.5-1$. But a complete history of dust-obscured energy production requires far-IR spectroscopy through the regime of peak activity in galaxies, to $z \sim 5$. This is only possible with a large, actively-cooled telescope and a zodiacal-light-limited grating spectrograph such as BLISS. We highlight some of these capabilities here.

2.1 Far-IR Spectroscopy as a Redshift Machine

The first measurements that spectroscopy with BLISS on SPICA will immediately provide are redshifts via the powerful fine-structure transitions of [SiII], [OI], [OIII], and [CII]. Did the dusty galaxies which produced the CIB undergo the same energy release history as the optically-selected populations? There is mounting evidence that the answer is no. A sample of the submm galaxies, which in principle are suffer very little redshift-selection bias, have redshifts 2–3 measured both with radio/optical follow-up,[7] and recently with the Spitzer IRS.[8,9] Similarly,

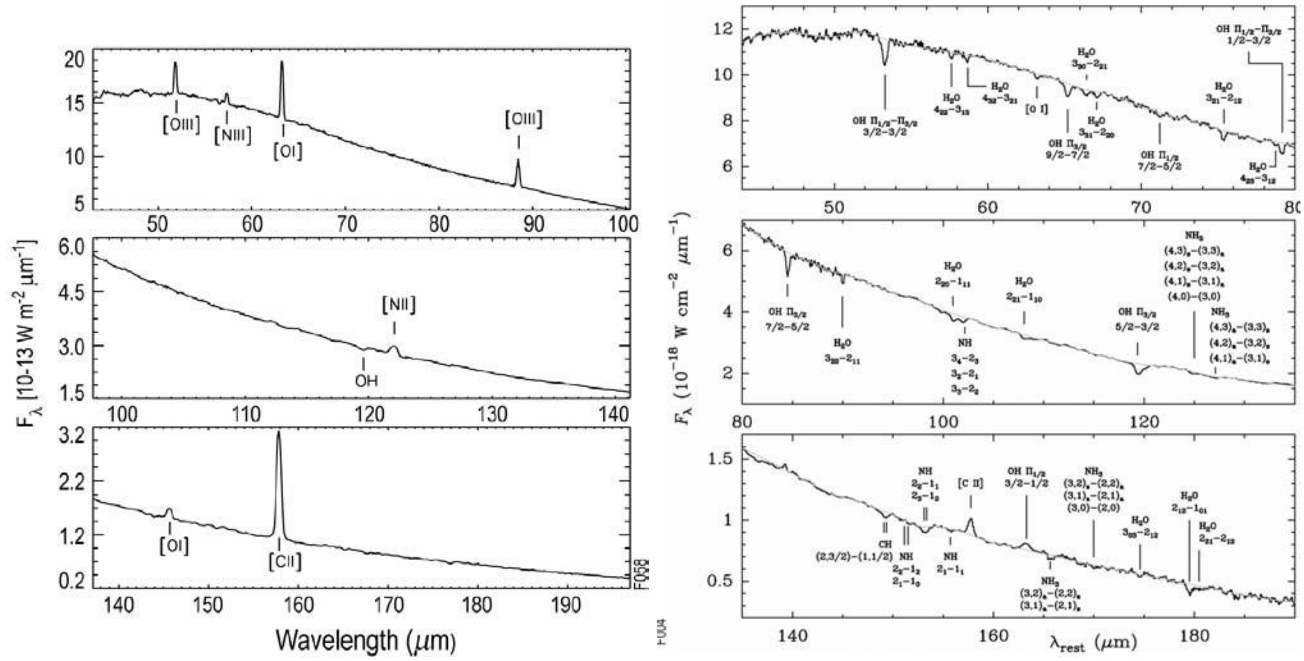

Figure 2. Far-IR spectra of nearby dusty galaxies obtained with the long-wavelength spectrometer (LWS) on board the Infrared Space Observatory. Left is the spectrum of the starburst galaxy M82 reprinted from Colber et al.,[5] and at right is the spectrum of the oft-studied ULIRG Arp 220 reprinted from Gonzalez-Alfonso et al.[6] Both emit the vast majority of their energy in the far-IR, and the variation between the two spectra is indicative of the wide range of properties in dusty galaxies. In M82, the fine-structure transitions are the primary coolants of the interstellar gas, and are among the most powerful spectral lines emitted by the galaxy. The suite of lines probes the conditions of the starburst, including the masses of the most massive stars. In Arp 220, the spectrum is dominated by absorption lines tracing the massive molecular reservoir which powers the star formation – in this case the OH absorption lines are among the most powerful spectral features. These galaxies are among only a handful of nearby galaxies which were accessible to the LWS; The spectrometers on Herschel will offer sensitivity to these lines in galaxies throughout the local universe to redshift of ∼0.5. But it is only with a cold telescope and a sensitive grating spectrometer such as BLISS that these types of measurements can be made on galaxies throughout their history.

the Spitzer 24-μm-selected sources confirm a dramatic decrease in luminosity from redshift 1 to the present: LeFloch et al.[10] infer a shift in characteristic luminosity L* at a rate of $(1+z)^{4.0\pm0.5}$, shown in Figure 1. Both the rapid evolution recently, and the potential peak between z ∼2–3 suggest that the far-IR-seletected dusty-galaxy populations may have had a different history from the optically-selected populations, which appear to have experienced a more constant rate of energy release with cosmic time.[11]

The BLISS-SPICA sensitivity of below $10^{-20}\,\mathrm{W\,m^{-2}}$ will enable follow-up of the LIRG- and ULIRG-class galaxies at redshifts 0.5–5 which likely produced the CIB in their dominant gas coolants: the powerful [OI], [OIII] and [CII] fine-structure transitions. These lines are the dominant coolants of the neutral ISM gas and HII regions, and each can carry to 1% of a galaxy's luminosity. The spectral coverage of BLISS ensures that at least two and generally more of these lines will fall in the band for all redshifts. The frequency ratio immediately identifies the lines and fixes the redshift for each galaxy. The survey sample could easily consist of a few thousand high-z galaxies, thus providing a statistically significant measure of properties when binned in both cosmic time ($\log(1+z)$: e.g.∼15 bins) and galaxy power ($\log L$: e.g. ∼6 bins). Based on the sensitivity estimated in Section 3.1, it is clear that survey will require less than one hour per galaxy on average, and if the initial redshift indications described above are appropriate, then BLISS-SPICA will access the vast bulk of the CIB populations.

2.2 The Far-IR Spectroscopic Toolbox

Even for the subset of dusty galaxies for which optical counterparts can be identified and optical spectra obtained, the high obscuration ensures that the optical spectra do not probe the bulk activity in these galaxies. It has

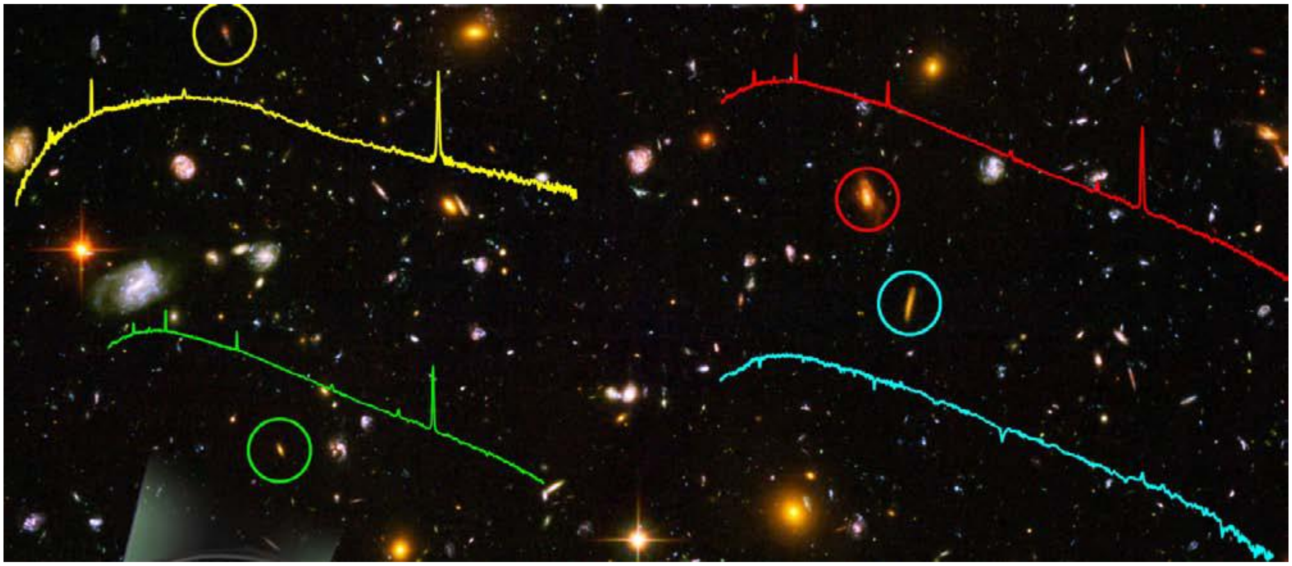

Figure 3. Hubble Ultra Deep Field with ISO Long Wavelength Spectrometer (LWS) spectra of nearby galaxies (Fischer et al., 1999). The spectra extend from 48 to 200 microns, a subset of the BLISS wavelength range for redshifts 0 to 3 (at higher redshifts, the longest wavelengths will be shifted into the ground-based submillimeter windows.) BLISS on SPICA will readily obtain spectra similiar to these but at higher spectral resolution galaxies and redshifted to as far as z$\sim$5. The circles show the BLISS-SPICA beamsize at 180 μm.

been shown that luminosities based on UV/blue fluxes and colors underestimate the total luminosities of a sample of LIRGs and ULIRGS by factors of 3–75, and that the UV/optical light often comes from regions hundreds of parsecs from the true luminosity sources.[12] Far-IR– submillimeter spectroscopy is the natural probe of astrophysics in dusty galaxies because it is immune to dust extinction, and therefore probes the entire galaxy. Unlike the mm-wave tracers available from the ground at longer wavelengths, the far-IR–submm transitions access all important components of interstellar gasmolecular, neutral atomic, and ionized. In this section we briefly ouline the wealth of astrophysical information available with the lines traced with SPICA in the far-IR.

Photo-dissociation Regions The UV radiation from newly-formed high-mass stars within molecular clouds strongly affects the natal molecular ISM. Within the immediate vicinity hydrogen is fully ionized forming an HII region whose size is set by cloud density and the number of H ionizing (Lyman continuum) photons that are available. Just beyond the HII region, far-UV (6 eV $<$ hν $<$ 13.6 eV) photons penetrate the neutral gas where they photoionize atoms and photo-dissociate molecules with ionization or dissociation potentials less than 13.6 eV forming photodissociation regions (PDRs). The depth of the PDR is determined by the extinction of far-UV photons by dust. Halfway through the PDR column, the far-UV field strength G is reduced to the extent that H_2 becomes selfshielding, and from this point further into the cloud, hydrogen is in molecular form. The heating of the gas in PDRs is primarily through the photo-electric ejection of energetic electrons from grains, with typical efficiency 1%. Most of the remaining stellar energy goes into heating the grains, which re-emit the energy in the far-IR continuum.[13] PDRs are an important ISM component–typically 10% by mass in normal Milky-Way-like galaxies, and up to 50% in starburst nuclei and low-metallicity dwarfs. The primary coolants of these dense PDRs, as well as moderate density atomic clouds are the [CII] 158 μm and [OI] 63 μm fine-structure lines. These lines are often the brightest single lines from star forming galaxies, each line can carry up to 1% of the total far-IR luminosity. Observing both lines together with the far-IR continuum constrains the physical conditions of the gas (temperature, density, mass), the area filling factor of the emitting gas region and the strength of the far-UV radiation field. The ionized gas close to the stars can be probed with line pairs (e.g. those of [NII], [SIII], [OIII]). These pairs directly measure density and thereby distinguish between between low-density HII regions associated with aging stellar populations, and the dense HII regions characteristic of young starbursts. Lines from different ionization states within an element (e.g. [OIII] & [OIV]; [NII] & [NIII]; [NeII], [NeIII], &

[NeV]) yield the hardness of the stellar radiation fields, hence identifying the masses of associated main-sequence stars. This is a measure of the age of the starburst, or its initial mass function. In addition, lines from different elements within a given ionization zone (e.g. [OIII] and [NIII]) yield relative elemental abundances, hence the history of stellar processing (e.g. Lester et al. 1987). An excellent example of the utility of the far-IR lines is that of Colbert et al.[5] shown in Figure 2. In this analysis the line fluxes are used to probe the starforming ISM and constrain the stellar populations in M82. The best fit is a 3–5 Myr burst with a 100 $M_\odot$ cutoff, and the line intensities require that half the total mass in the central few hundred pc is involved in the starburst. BLISS-SPICA will the wavelength coverage and sensitivity to make these kind of measurements on LIRG-class galaxies from redshift of 3, when the universe was 1/6 its current age, to the present day.

Dense Molecular Gas: Rotational Transitions of Hydrides and High-Excitation CO The far-IR and submillimeter is also the waveband which carries the dominant coolants of the molecular gas. In the Milky Way and nearby galaxies, UV-shielded molecular gas accounts for about half of the interstellar medium by mass. Since it is the birthplace of stars, understanding the heating and cooling of molecular gas constrains theories of star formation. For typical molecular material, CO is regarded as the most important coolant, and $J = 1 \rightarrow 0$, $J = 2 \rightarrow 1$, and $J = 3 \rightarrow 2$ transitions have been the standard measure of molecular gas mass due to their accessibility. However, observations up to $J = 7 \rightarrow 6$ the highest-frequency transition accessible from the ground now show that much of the molecular gas in starburst galaxies is heated to 100 K or more by stellar UV, turbulence, or cosmic rays.[14,15] This implies that the $J \leq 7$ lines alone are insufficient probes of the temperature, energetics, or mass of the molecular gas in these cases. The mid-J (J=8–15) far-IR CO transitions accessible to BLISS at low to moderate redshift are a critical complement to the ground-based observations to reveal the full molecular gas energy budget. For even more extreme molecular material such as that associated with protostellar condensations, shock-excited gas, and AGN tori, the dominant coolants are the light hydrides: OH, CH, and H_2O, and high-J CO. The hydrides have rotational fundamentals in the far-IR, and rapid radiative rates. In the dustiest of galaxies in the local universe, these lines are often seen in absorption, providing a direct measure of column densities and abundances of optically thin species, as shown for Arp 220[6] in Figure 2. In particular for the torus around an AGN, the high-J CO lines are expected to be very important coolants due to the high density ($10^7\,\mathrm{cm}^{-3}$) and temperature ($\sim$1000 K). Krolik and Lepp[16] estimate that in these extreme regions, a single CO line (e.g. $J{=}40{\rightarrow}39$) at 70 μm can have up to 1% of the input X-ray flux, making it detectable with BLISS-SPICA at redshift 2 for a luminous AGN.

2.3 Interstellar Medium Conditions at z$\sim$1–5

At high redshift, the process of star formation and perhaps the conditions around massive black holes are likely to be modified by the lower metallicity of the interstellar medium, as well as potential differences in the structure of typical galaxies. For example, the dust to gas ratio decreases with decreasing metal content.[17,18] and this trend has been invoked to explain differences in the global infrared SEDs of ULIRGs at z$\sim$2.[19] In addition, the morphologies of high-redshift infrared galaxies indicate that many of them are not major mergers (as are most local ULIRGs) but appear to be only modestly disturbed spirals.[20,21] These observations suggest that local analogs do not represent well the conditions in the dominant IR galaxy population at high redshift. There are no local low-metallicity ULIRGs and the great majority of local star-forming ULIRGs are dominated by nuclear-concentrated regions of extremely high optical depth in dust. The conditions in the ISM not only affect the observed properties of galaxies, they also strongly influence the processes that lead to star formation. Optical spectroscopy (probing the rest frame UV) is so strongly affected by extinction that it cannot give a representative view of a high-redshift ISM, while sensitivity limitations make detailed observations in the near-IR (rest optical) impossible. The strong, extinction-free, and highly diagnostic complex of lines accessible in the far-IR are the best observables to support astrophysical analyses of the conditions in the interstellar gas in these galaxies.

2.4 Source Confusion for Far-IR Spectroscopy with BLISS / SPICA

Source confusion has been a major limitation in traditional direct broadband imaging and highredshift source extraction at the long far-IR wavelengths. However, simple arguments show that the spectroscopic observations that we envision for BLISS on SPICA will not be limited in the same way. The key difference is that unlike a

Table 1. BLISS Instrument Bands, Modules Sizes, and Detector Formats

Band	λ_{min} μm	λ_{max} μm	L cm	W cm	H cm	N_{det}	Spat. Pitch μm	Spec. Pitch μm
Cross-dispersed echelle modules								
1	38	67	10.3	6.6	6.0	960 ×2	306	193
2	67	116	18.0	11.5	11.0	960 ×2	535	337
WaFIRS modules								
3	116	180	14.9	14.9	3	768 ×2	873	140
4	180	280	23.1	23.1	4	768 ×2	1353	216
5	280	433	35.9	35.9	4	768 ×2	2097	336
Total Envelope, both beams								
	38	433	50	50	50	4224		

continuum flux, the spectral information produces a meaningful signal when differenced from a nearby reference position. Our survey does not require sources to be extracted based on their brightness relative to the aggregate background, but instead to follow up known sources with positions determined by other means. The sources will be based on shorter-wavelengths images. In practical terms the space density of BLISS sources will be similar to the space density of sources in the surveys which are resolving the bulk of the galaxy populations. A prime example is the Spitzer 24-μm populations. The source density is on order 15 per square arcminute.[22,23] This means that there will be on average 0.5 sources per 200 μm BLISS-SPICA beam. This density is too high for this source to produce a signal in a continuum map, because the broadband flux in the target beam is nearly indistinguishable from the flux in adjacent beams. However, because the spectral lines will vary from beam to beam, a source density of order unity will be adequate to ensure that the spectral information gathered belongs with the intended 24 μm source. A sanity check is Figure 3 which shows a Hubble Deep Field image with appropriately-sized BLISS beams overlaid. Even in this very deep optical image, it is clear that with careful sample selection, it will be possible to follow-up many galaxies unambiguously.

3. BLISS APPROACH, ARCHITECTURE

3.1 Fundamental limits to far-IR observations

Substantial gains are still possible in the far-IR because existing far-IR spectroscopy platforms operate far from the ultimate sensitivity limitation: photon noise from the diffuse astrophysical background. The background is produced by interplanetary and interstellar dust, the cosmic far-IR background and the CMB. Careful analysis of COBE DIRBE data[24,25] has revealed the components, and it is straightforward to calculate the resulting sensitivities. As Figure 4 shows, in regions of low zodiacal light , the photon noise on a cold telescope can be four orders of magnitude lower than that produced by a passively-cooled ($\sim$80 K) telescope. A cryogenic 3-meter class telescope with a dispersive BLISS spectrometer is capable of probing ULIRG-type sources out to redshifts of 5, and the sensitivity increase translates into factors of more than 10^6 speed improvement in obtaining a complete spectrum for a distant galaxy.

3.2 BLISS Technical Approach

The philosophy of BLISS is based on the aims of the scientific investigation outlined above: broadband follow-up spectroscopy of unresolved sources with known positions. The instrument therefore aims to provide maximum sensitivity at moderate resolving power with complete instantaneous spectral coverage. Spatial multiplexing (imaging/mapping) is a secondary goal. Heterodyne spectrometers are not well-suited to cold space telescopes because they suffer from quantum noise—a term that is factors of 100–1000 times greater than the photon noise from the natural backgrounds. Moreover, the heterodyne backend bandwidths are insufficient for effective spectral surveying. Direct-detection spectrometers are the natural choice, and the broad bandwidth requirement permits two basic options: diffraction gratings and Fourier-transform spectrometers (FTS). With suitable detectors, the grating spectrometer is more sensitive for observations of a single point source. BLISS is therefore a broadband grating, optimized in this way. The sensitive spectroscopic capability is complementary with the 2-D survey capability of SAFARI, the FTS under study by the European consortium.[3]

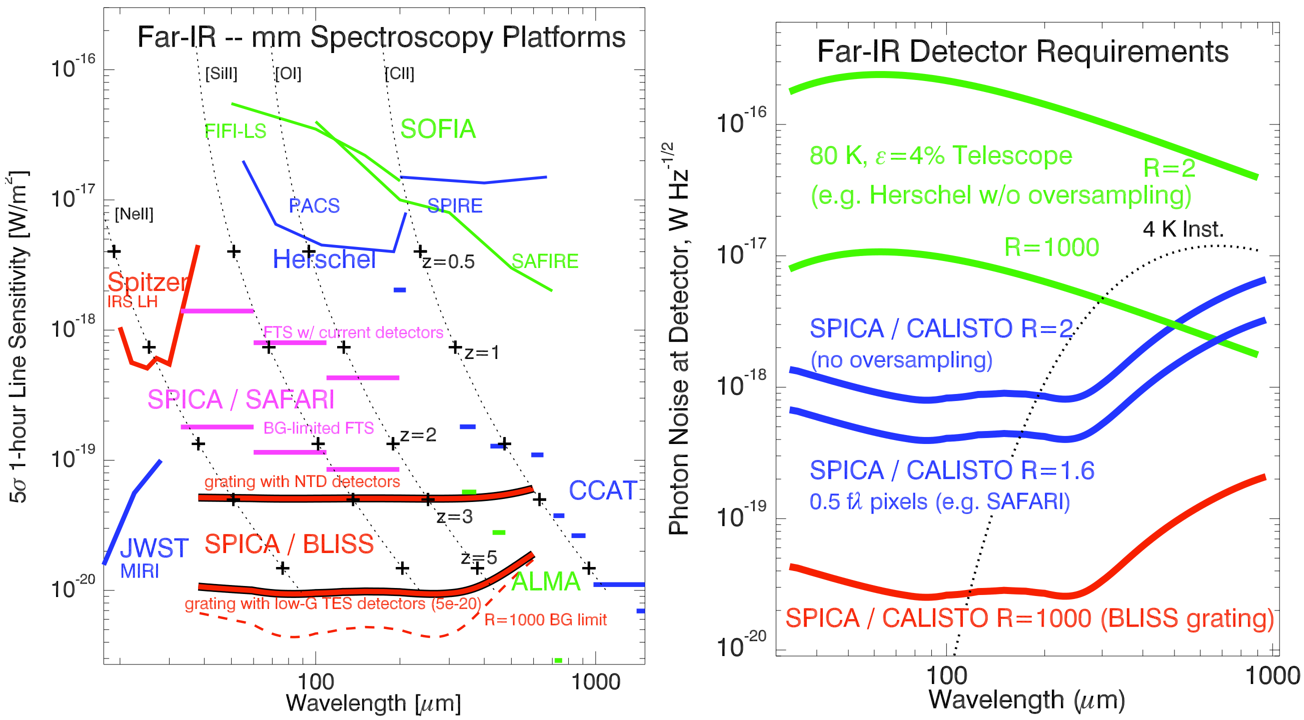

Figure 4. RIGHT: Sensitivity of far-IR spectroscopy platforms. Values for SOFIA, Herschel, Spitzer, and ALMA are taken from the instrument web pages. For ALMA, we assume a 300 km/s linewidth. The blue CCAT curves represent the background-limited R=1000 spectrometers on the proposed 25-m Cornell-Caltech Atacama Telescope at a high site. The SPICA-SAFARI curves are taken from the SAFARI literature. The red SPICA-BLISS curves are calculated assuming a 3.5-meter telescope with 75% aperture efficiency and 25% total instrument transmission in a single polarization, and assume that the source is compared with a reference as required with bolometers. Sky backgrounds are average values appropriate for the North Ecliptic Pole. The light dashed curved at bottom shows the photon background limit, the heavy curve above it assumes a detector noise-equivalent power (NEP) of 5×10^{-20} W Hz$^{-1/2}$, achievable with transition-edge superconducting bolometers, and the upper red curve shows the performance possible with semiconducting (NTD Germanium)-sensed bolometers which could achieve an NEP of 3×10^{19} W Hz$^{-1/2}$. As a guide to the astronomical capability, overplotted are spectral line intensities from ULIRG at various redshifts assuming a fractional line intensity of 10^{-3}, and the current cosmology ($\Omega_{vac} = 0.73$, $\Omega_{mat} = 0.27$, $H_0 = 71$). LEFT: Detector requirements for far-IR platforms. The grating spectrometer requires detectors with NEPs well below anything built to date.

A single grating spectrometer only efficiency couples a single octave of bandwidth, so the full BLISS instrument is actually a series of spectrometer modules presented in Table 1. The original BLISS concept was R∼1000 in six bands, extending to 670 μm the current working concept for BLISS is now reduced given the stringent mass limitations on SPICA. BLISS is now five bands at R∼700, extending to 433 μm. We have eliminated the longest-wavelength band (λ = 430–720 μm), and have reduced the resolving power to R=700. The loss of the submillimeter band is reasonable given the capabilities of the ground-based facilities shown in Figure 4. The reduction of the resolving power will have a small impact on the scientific performance, but since the linear dimension is reduced by 70%, the volume and mass are reduced by at least a factor of 2, a substantial savings. The total estimated mass of the cold BLISS instrument, including the spectrometer modules, refrigerator, and associated shields and supports is 50 kg.

BLISS will employ two types of broadband grating spectrometer. The WaFIRS system demonstrated at $\lambda = 1\,mm$ will be used for the longer wavelengths. WaFIRS is a 2-D system which uses a custom-machined curved grating in parallel plate waveguide – its principal advantage is the compact size. For the shorter wavelengths, BLISS will employ a cross-dispersed echelle grating modules, similar to those employed for the high-resolution modules of the Spitzer IRS, using an ultra-compact design. Both are shown in Figure 5, and described more fully in the previous SPIE paper.[4] The trade between the two approaches is essentially that the waveguide

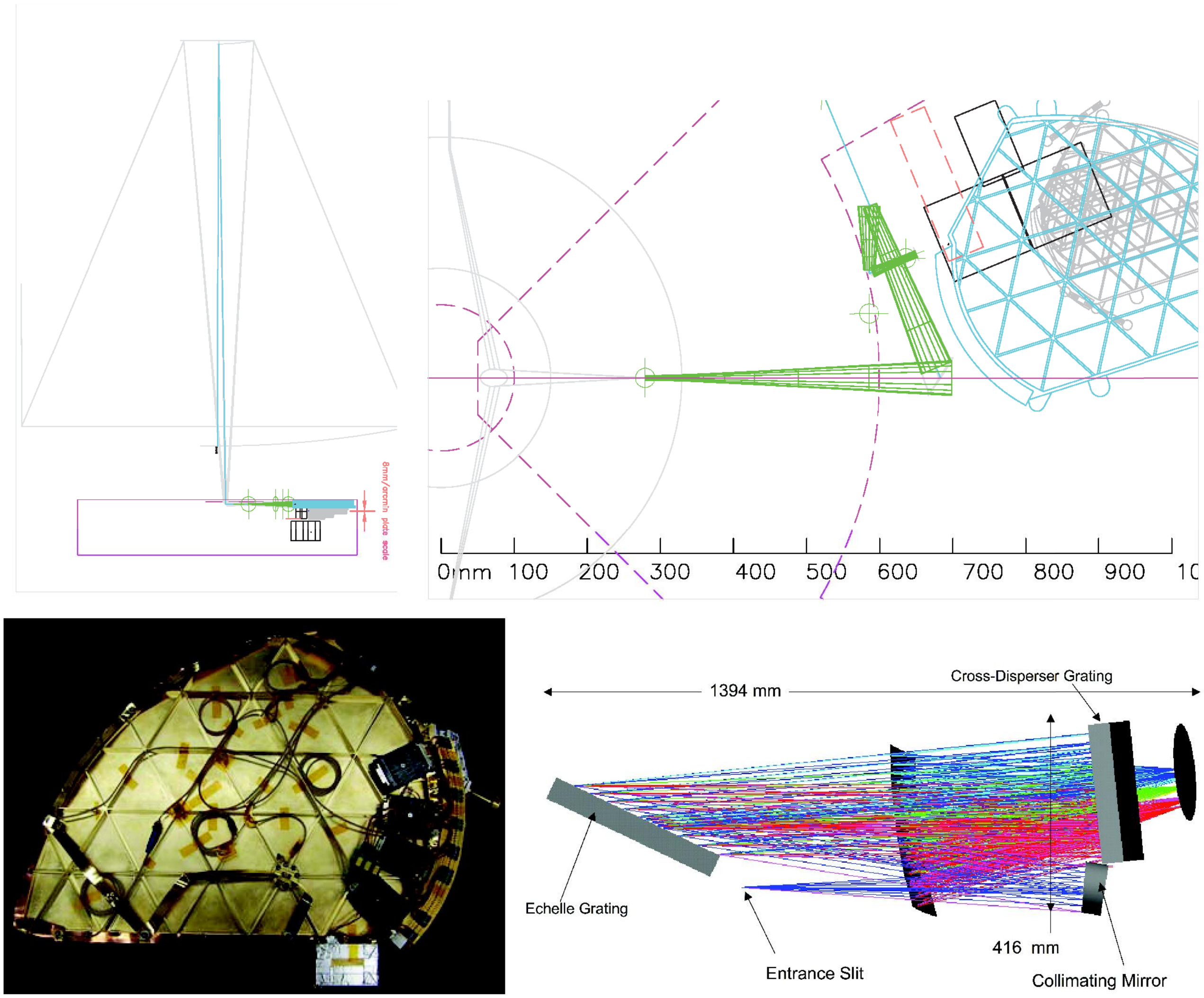

Figure 5. Top: Proposed layout of the BLISS modules in the SPICA instrument envelope. A pickoff mirror relays an off-axis field to the instrument, which sits 65 cm from the telescope boresight. This offset allows the shorter-wavelength instruments to access the telescope boresight region. Bottom: Spectrograph approaches for BLISS: on the left is the Z-Spec $\lambda = 1\,\mathrm{mm}$ demonstration of the planar waveguide spectrometer which will be used for the longer wavelengths, on the right is the cross-dispersed echelle spectrograph design for BLISS. For both, the linear dimensions scale with $\lambda \times R$ (with offsets) and the resulting dimensions are provided in Table 1 . Both are described more fully in the previous proceeding.[4]

system is more compact and thus less massive for a given $\lambda \times R$ product, but requires fabrication and assembly of waveguide parts with tolerances on order $\lambda/20$. The echelle approach is adopted for the shorter wavelengths where volume is not a constraint, and the waveguide approach is adopted for the long wavelengths where the echelle would be too large and massive.

BLISS will couple two beams on the sky, one in each bank of spectrometers. A given sky position will be interchanged between the two spectrometer banks with a cryogenic chopping mirror, the third mirror in the Figure 5 layout. This provides the necessary modulation for the bolometric measurement. The chopper is at an image of the secondary, which minimizes differential spillover between the chop positions and is mounted to the 4 K chassis. The chopper mirror is curved, saving one mirror and reducing beam aberration and cross-polarization relative to the comparably compact 3-mirror configuration (flat chopper between two curved mirrors). The spectrometer input feedhorns are separated by Heritage for the chopper exists (e.g. Herschel HIFI), and it is

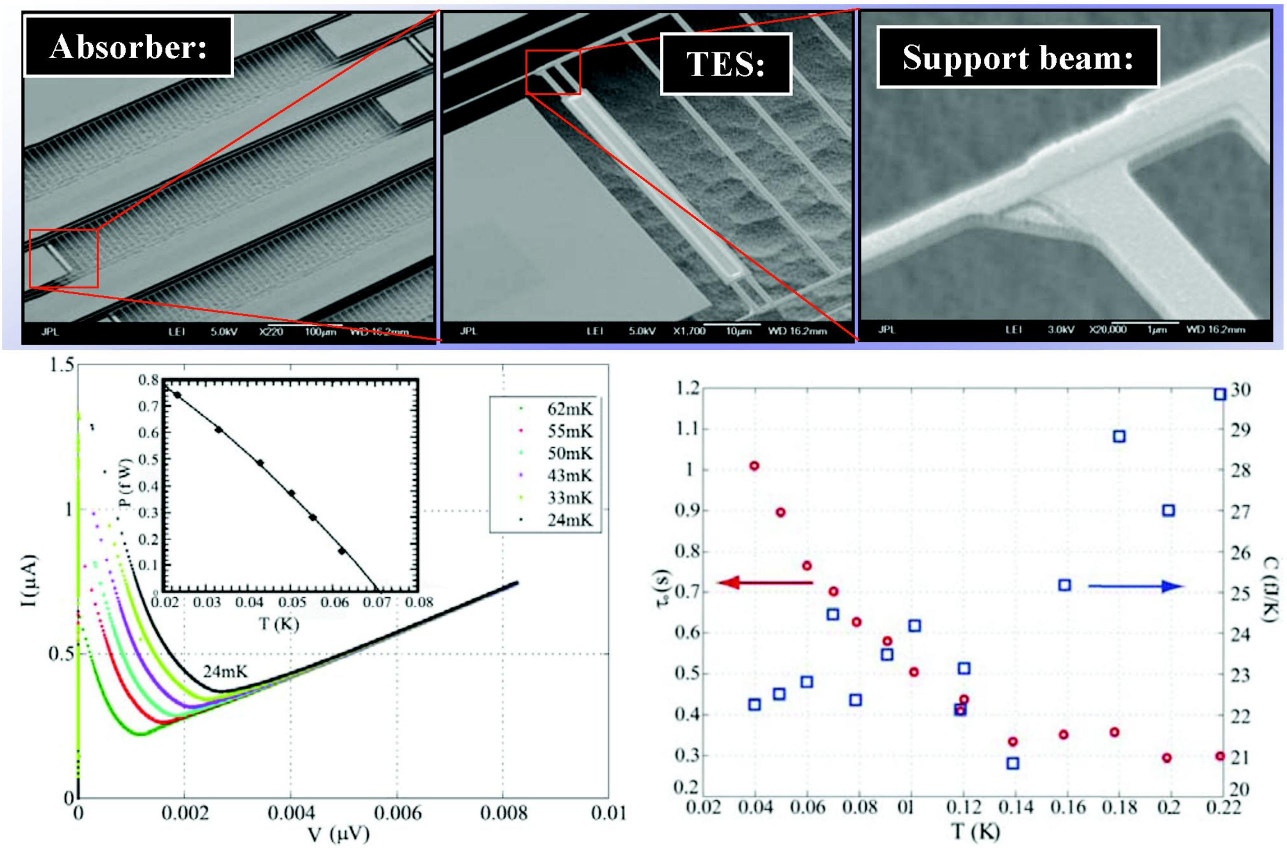

Figure 6. Latest results from the low-G TES program at JPL's Microdevices Lab (MDL). TOP: Micrograph of TESs with 500 μmlong by 75 μm-wide absorbers (see left micrograph) and 1000 μm-long by 0.25 μm-thick by 0.4 μm-wide support beams (see right micrograph). (Note: the beams extend beyond the edge of the micrograph.) The thermistors are Mo/Au bilayer films deposited onto SixNy and Al wires runs along the support beams connecting the thermistor to the SQUID readout (see middle micrograph). The final release of the SixNy structure is performed using a XeF_2 etcher which causes the Si underneath the SixNy support structure to appear pitted. (In this array, wire grid absorber devices alternate with membrane devices for testing of the heat capacity). BOTTOM LEFT: I-V characteristic for a range of temperatures for a TES with support beams with a similar length to cross-section aspect ratio as those above. Inset: Electrical bias power through the TES as a function of mixing chamber temperature. The solid line is a power-law fit to the data with an exponent equal to 1.43. A thermal conductance G of 19 pW/K and a transition temperature of T_c=71 mK for the Mo/Au thermistor is determined by the slope and x-intercept of the line, respectively. BOTTOM RIGHT: "Natural" response time τ_0 (red circles) as a function of temperature T for a typical leg-isolated detector structure (without TES thermistor) measured with a normal-metal resistor, i.e. without electrothermal feedback. The time constant is less than a second. With the addition of electrothermal feedback, we anticipate a speed-up by a factor of at least 10, making the device fast enough for BLISS at 50 mK. By measuring the natural response time, we can calculate the heat capacity of the absorber, shown as blue squares referred to the right axis.

anticipated that the modest requirements for variable chopper period (0.5–10 sec), duty cycle (>90%), and throw (1–3 arcmin on the sky) will not significantly impact the design. Based on this heritage, we estimate that the chopper will dissipate 0.5 mW on the 4 K stage, a negligible impact on SPICA's thermal budget.

4. DETECTORS FOR BLISS

Detectors for BLISS an the future far-IR flight spectrometers will be unlike anything built thus far for the far-IR (see Figure 4). Background loadings are factors of 10^4 to 10^6 times lower than for ground-based-and Herschel instruments for which the warm telescope emission dominates the astrophysical backgrounds. The detector requirements for BLISS and the future background-limited spectrometers are set by the detector bandwidth and by the backgrounds at L2 and are independent of the telescope aperture. For continuum imaging for Fourier-transform-type spectroscopy, the required NEP is on the order of $10^{-19}\,\mathrm{W\,Hz^{-1/2}}$ and is comparable to ground-based submillimeter and millimeter-wave spectrometers (Z- Spec, SPIFI, ZEUS, FIBRE) and the 70 μm array in Spitzer MIPS. Achieving the ultimate capability of BLISS-SPICA and SAFIR/CALISTO, however, requires dispersive spectroscopy, for which the photon-limited NEP is a few times $10^{-20}\,\mathrm{W\,Hz^{-1/2}}$.

While there are several promising new technologies under development, the most suitable approach given SPICA's timescale is to array superconducting transition-edge-sensed bolometers with a SQUID based multiplexing readout (MUX). This technology has seen significant progress in the last few years; current and future deployment of arrays of 1000's of membrane-isolated TESs are underway, and it is straightforward to build efficient wire-grid absorber-coupled TESs from 40 μm to 600 μm. However, to reach an extremely low NEP of a few$\times 10^{-20}\,\mathrm{W\,Hz^{-1/2}}$, one must reduce the fundamental intrinsic temperature-fluctuation noise due to phonon fluctuations between the absorber of the bolometer and the substrate. The expression for this noise is: $\mathrm{NEP_{phonon}} = \sqrt{\gamma 4 \mathrm{k} \mathrm{T}^2 \mathrm{G}}$, where G is the thermal conductance between the absorber and the substrate, T is the bolometer temperature, and γ is a factor of order unity. As discussed in Section 5, our group is developing a cooler based on an ADR which can provide lift at 50 mK. At this base temperature, one must reduce G to $\sim$10 fW/K to obtain the required NEP of $\sim$few$\times 10^{-20}\,\mathrm{WHz^{-1/2}}$.

While achieving such low NEP is challenging, our group has built single-pixel TESs and shown that they are sensitive and fast enough for BLISS.[26] In particular, we have built TESs consisting of a superconducting thermistor patterned onto a suspended, thermally isolated absorber that is connected to the substrate through four SixNy support beams (see Figure 6, top). By making the aspect ratio of the length-to-cross-sectional area of the support beams very large, we have shown that G can be lowered to about 10 fW/K (Figure 6, bottom), as required for BLISS. *This is roughly 1000 times lower than the G needed for all astrophysics applications to date which use bolometers for observations in the far-IR/submm/mm.*

One may be concerned that ultra-sensitive TESs may be too slow for practical use because the response time is given by the ratio of the heat capacity C to the G, $T \sim C/G$. However, we have measured the response, and showed that by reducing the thermal mass of the absorber and relying on electrothermal feedback, TESs can be made fast enough for BLISS. We measured the effective response time τ of a low-G island (without a TES) (see Fig 6). We performed the measurement by coupling optical pulses from an LED through an optical fiber into the sample box of the TES. The natural response time of these devices is less than 1 second, and this should be reduced by a factor of at least 10 with a voltage-biased TES thermistor. This is suitable for BLISS. Since BLISS will operate in a simple spatial chopping mode, the detector speed requirement is determined only by the need to avoid low-frequency noise. This will of course depend on the details of the environment on board SPICA, and its interaction with the TESes, but we anticipate that a 100-ms time constant should be suitable. We note that the measured heat capacity is much larger than predicted with simple Debye-type lattice models and electronic contributions. We are currently investigating the device heat capacity and studying ways to reduce it further.

5. BLISS SUB-K COOLING, THERMAL ARCHITECTURE

In light of the very low NEP detectors required for BLISS ($\sim 5 \times 10^{-20}\,\mathrm{W\,Hz^{-1/2}}$), and the corresponding very low optical loading ($\sim 10^{-18}\,\mathrm{W}$) on the detector, all of the BLISS focal plane modules will have to be cooled to T$\sim$50 mK. This is a challenge, especially given the heat lift limitation of SPICA (5 mW at 1.7 K). The current state-of-the-art sub-Kelvin flight coolers is limited to ^{3}He sorption coolers on IRTS and Herschel/SPIRE ($> 280\,\mathrm{mK}$ in a single shot mode), the Planck open-cycle dilution refrigerator (100 mK, <200 nW, 2.5 year life due to expendables), and the ASTRO-E Adiabatic Demagnetization Refrigerator (ADR) (60mK, single shot). All cooled cold stages with mass <2 kg, much smaller than BLISS. Thus there are no proven coolers capable of meeting the requirements for BLISS. The ^{3}He sorption systems are not cold enough, and the open cycle dilution fridge cannot approach the 5-year life in any practical configuration. A scaled version of the ASTRO-E ADR appropriate for BLISS would exceed SPICA's heat lift capability.

A major improvement to any 50 mK ADR system staging from $T > 1$K is to include an intercept stage at T$\sim$500 mK. Such a dual-stage system could cool a smaller version of BLISS in single-shot mode, with a reasonable mass ($\sim$8 kg). However, the duty cycle of a single-shot system is limited; for this cooler, the duty

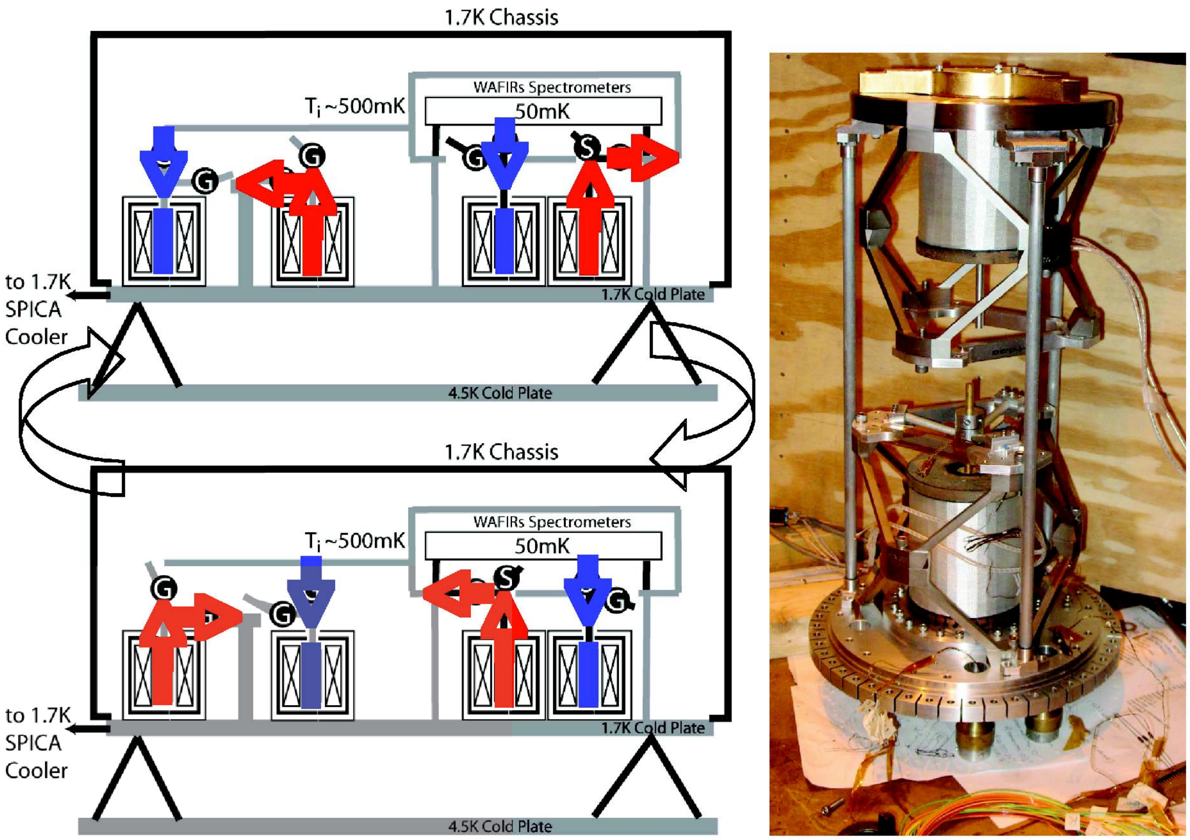

Figure 7. LEFT: Schematic of 2-stage continuous ADR envisioned for BLISS. The blue rectangles represent paramagnetic salt pills absorbing heat at operational temperature; the red indicate pills which are dumping heat while recycling to the next higher temperature stage. Arrows indicate power flow. The upper and lower frames represent the two phases of the operational cycle. RIGHT: Prototype hardware: a single-shot dual stage system to verify salt pills and parasitic loads.

cycle in cooling the full BLISS instrument outlined above would be below 50%, an unacceptable observing efficiency. A continuous ADR is the only way to achieve reasonable duty cycle in a modest cooler mass for a spectrograph such as BLISS. Continuous cooling can be achieved from a proper configuration of multiple salt pills and heat switches, shown schematically in Figure 7. Such a system is ideal for long-duration missions; only electrical power is required, there are no expendables and no moving parts.

We have developed such a concept for cooling the BLISS spectrometers to 50 mK. The specifications begin with the thermal loads on the cold stage, estimated to be 1.6 μW, primarily the parasitic load conducted through the titanium suspension, but with a contribution from the SQUIDs on the detector stage. This parasitic would be much higher if not for the intercept stage at 0.5 K, which intercepts 33 μW from higher-temperature stages. The four pills and magnets (each with multi-layer magnetic shielding), along with the required copper straps and heat switches have a mass of 14 kg and the system exhausts between 1 and 3 mW of power to SPICA's 1.7 K cooler. The other system-level parasitics required of the ADR are due to the magnet leads, which must carry up to 6.5 Amps. The baseline approach for this is to use brass leads from the warm spacecraft to 85 K, then high-T_C superconducting leads below 85 K, then NbTi superconducing leads below 4 K to the magnets at 1.7 K. We have optimized the size of the magnet wires between each of SPICA's thermal shields to minimize the total parasitic + ohmic heat load. At each temperature stage, the optimized magnet leads present additional loads of less than 10% of the nominal parasitics in the current SPICA cryogenic design.[27]

REFERENCES

1. Matsuhara, H. and Kataza, H., "Focal plane instruments onboard SPICA," in [*Proc. SPIE*], **7010** (July 2008).

2. Nakagawa, T., "SPICA mission for mid- and far-infrared astronomy," in [*Proc. SPIE*], **7010** (July 2008).
3. Swinyard, B. and Nakagawa, T., "European contribution to the SPICA mission," in [*Proc. SPIE*], **7010** (July 2008).
4. Bradford, C. M. in [*Proc. SPIE*], **6265** (July 2006).
5. Colbert, J. W. and others, "ISO LWS Spectroscopy of M82: A Unified Evolutionary Model," *Astrophys. J.* **511**, 721–729 (Feb. 1999).
6. González-Alfonso, E., Smith, H. A., Fischer, J., and Cernicharo, J., "The Far-Infrared Spectrum of Arp 220," *Astrophys. J.* **613**, 247–261 (Sept. 2004).
7. Chapman, S. C., Blain, A. W., Smail, I., and Ivison, R. J., "A Redshift Survey of the Submillimeter Galaxy Population," *Astrophys. J.* **622**, 772–796 (Apr. 2005).
8. Valiante, E. and others, "A Mid-Infrared Spectroscopic Study of Submillimeter Galaxies: Luminous Starbursts at High Redshift," *Astrophys. J.* **660**, 1060–1071 (May 2007).
9. Pope, A. and others, "The Hubble Deep Field-North SCUBA Super-map - IV. Characterizing submillimetre galaxies using deep Spitzer imaging," *Mon. Not. Roy. Astron. Soc.* **370**, 1185–1207 (Aug. 2006).
10. Le Floc'h, E. and others, "Infrared Luminosity Functions from the Chandra Deep Field-South: The Spitzer View on the History of Dusty Star Formation at 0<z<1," *Astrophys. J.* **632**, 169–190 (Oct. 2005).
11. Hopkins, A. M. and Beacom, J. F., "On the Normalization of the Cosmic Star Formation History," *Astrophys. J.* **651**, 142–154 (Nov. 2006).
12. Goldader, J. D., Meurer, G., Heckman, T. M., Seibert, M., Sanders, D. B., Calzetti, D., and Steidel, C. C., "Far-Infrared Galaxies in the Far-Ultraviolet," *Astrophys. J.* **568**, 651–678 (Apr. 2002).
13. Hollenbach, D. J. and Tielens, A. G. G. M., "Dense photodissociation regions (PDRs)," *Annual Review of Astronomy and Astrophysics* **35**(1), 179–215 (1997).
14. Bradford, C. M. and others, "CO (J=7–6) Observations of NGC 253: Cosmic-Ray-heated Warm Molecular Gas," *Astrophys. J.* **586**, 891–901 (Apr. 2003).
15. Weiß, A., Downes, D., Neri, R., Walter, F., Henkel, C., Wilner, D. J., Wagg, J., and Wiklind, T., "Highly-excited CO emission in APM 08279+5255 at z = 3.9," *Astron. Astrophys.* **467**, 955–969 (June 2007).
16. Krolik, J. H. and Lepp, S., "The physical state of the obscuring torus in Seyfert galaxies," *Astrophys. J.* **347**, 179–185 (Dec. 1989).
17. Draine, B. T. and others, "Dust Masses, PAH Abundances, and Starlight Intensities in the SINGS Galaxy Sample," *Astrophys. J.* **663**, 866–894 (July 2007).
18. Engelbracht, C. W. and others, "Metallicity Effects on Dust Properties in Starbursting Galaxies," *Astrophys. J.* **678**, 804–827 (May 2008).
19. Rigby, J. R. and others, "Mid-Infrared Spectroscopy of Lensed Galaxies at between z=1 and z=3: The Nature of Sources Near the MIPS Confusion Limit," *Astrophys. J.* **675**, 262–280 (Mar. 2008).
20. Bell, E. F. and others, "Dry Mergers in GEMS: The Dynamical Evolution of Massive Early-Type Galaxies," *Astrophys. J.* **640**, 241–251 (Mar. 2006).
21. Lotz, J. M., Madau, P., Giavalisco, M., Primack, J., and Ferguson, H. C., "The Rest-Frame Far-Ultraviolet Morphologies of Star-forming Galaxies at z ˜ 1.5 and 4," *Astrophys. J.* **636**, 592–609 (Jan. 2006).
22. Chary, R. and others, "The Nature of Faint 24 Micron Sources Seen in Spitzer Space Telescope Observations of ELAIS-N1," *Astrophys. J. Supp. Ser.* **154**, 80–86 (Sept. 2004).
23. Papovich, C. and others, "The 24 micron source counts in deep Spitzer Space Telescope surveys," *Astrophysical Journal Supplement Series* **154**, 70–74 (Sept. 2004).
24. Kelsall, T. and others, "The COBE Diffuse Infrared Background Experiment Search for the Cosmic Infrared Background. II. Model of the Interplanetary Dust Cloud," *Astrophys. J.* **508**, 44–73 (Nov. 1998).
25. Arendt, R. G. and others, "The COBE Diffuse Infrared Background Experiment Search for the Cosmic Infrared Background. III. Separation of Galactic Emission from the Infrared Sky Brightness," *Astrophys. J.* **508**, 74–105 (Nov. 1998).
26. Kenyon, M., Day, P., Bradford, C., Bock, J., and LeDuc, H. *J. Low Temp. Physics* **151**, 112–118 (Jan. 2008).
27. Sugita, H., Nakagawa, T., Murakami, H., Okamoto, A., Nagai, H., Murakami, M., Narasaki, M., and Hirabayashi, M., "Cryogenic infrared mission "JAXA/SPICA with advanced cryocoolers," *Cryogenics* **46**, 149–157 (Mar. 2006).